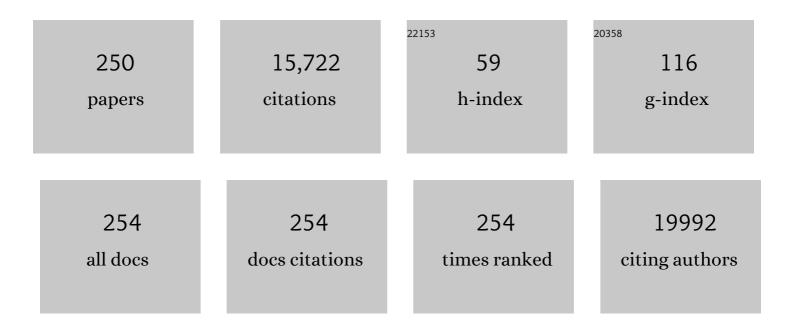
Xiaoping Shen

List of Publications by Year in descending order

Source: https://exaly.com/author-pdf/7356126/publications.pdf Version: 2024-02-01



#	Article	IF	CITATIONS
1	Graphene nanosheets for enhanced lithium storage in lithium ion batteries. Carbon, 2009, 47, 2049-2053.	10.3	1,281
2	Synthesis and characterisation of hydrophilic and organophilic graphene nanosheets. Carbon, 2009, 47, 1359-1364.	10.3	565
3	Graphene–inorganic nanocomposites. RSC Advances, 2012, 2, 64-98.	3.6	547
4	Hydrogels based on cellulose and chitin: fabrication, properties, and applications. Green Chemistry, 2016, 18, 53-75.	9.0	522
5	In situ chemical synthesis of SnO2–graphene nanocomposite as anode materials for lithium-ion batteries. Electrochemistry Communications, 2009, 11, 1849-1852.	4.7	520
6	Synthesis of enhanced hydrophilic and hydrophobic graphene oxide nanosheets by a solvothermal method. Carbon, 2009, 47, 68-72.	10.3	446
7	Solvothermal synthesis of NiCo-layered double hydroxide nanosheets decorated on RGO sheets for high performance supercapacitor. Chemical Engineering Journal, 2015, 268, 251-259.	12.7	401
8	Hydrothermal Synthesis and Optical, Magnetic, and Supercapacitance Properties of Nanoporous Cobalt Oxide Nanorods. Journal of Physical Chemistry C, 2009, 113, 4357-4361.	3.1	374
9	Fe ₃ O ₄ â€Decorated Co ₉ S ₈ Nanoparticles In Situ Grown on Reduced Graphene Oxide: A New and Efficient Electrocatalyst for Oxygen Evolution Reaction. Advanced Functional Materials, 2016, 26, 4712-4721.	14.9	348
10	Vascular and inflammatory stresses mediate atherosclerosis via RAGE and its ligands in apoE–/– mice. Journal of Clinical Investigation, 2008, 118, 183-194.	8.2	325
11	One-pot solvothermal preparation of magnetic reduced graphene oxide-ferrite hybrids for organic dye removal. Carbon, 2012, 50, 2337-2346.	10.3	321
12	Solvothermal synthesis and characterization of sandwich-like graphene/ZnO nanocomposites. Applied Surface Science, 2010, 256, 2826-2830.	6.1	310
13	Reduced graphene oxide/nickel nanocomposites: facile synthesis, magnetic and catalytic properties. Journal of Materials Chemistry, 2012, 22, 3471.	6.7	273
14	Nitrogen-doped carbon dots decorated on g-C3N4/Ag3PO4 photocatalyst with improved visible light photocatalytic activity and mechanism insight. Applied Catalysis B: Environmental, 2018, 227, 459-469.	20.2	258
15	Solvothermal synthesis and gas-sensing performance of Co3O4 hollow nanospheres. Sensors and Actuators B: Chemical, 2009, 136, 494-498.	7.8	185
16	CoP nanoparticles deposited on reduced graphene oxide sheets as an active electrocatalyst for the hydrogen evolution reaction. Journal of Materials Chemistry A, 2015, 3, 5337-5343.	10.3	181
17	Facile Fabrication and Enhanced Sensing Properties of Hierarchically Porous CuO Architectures. ACS Applied Materials & Interfaces, 2012, 4, 744-751.	8.0	171
18	In situ Growth of Ni _{<i>x</i>} Co _{100–<i>x</i>} Nanoparticles on Reduced Graphene Oxide Nanosheets and Their Magnetic and Catalytic Properties. ACS Applied Materials & Interfaces, 2012, 4, 2378-2386.	8.0	152

#	Article	IF	CITATIONS
19	Nanocomposites Based on CoSe ₂ -Decorated FeSe ₂ Nanoparticles Supported on Reduced Graphene Oxide as High-Performance Electrocatalysts toward Oxygen Evolution Reaction. ACS Applied Materials & Interfaces, 2018, 10, 19258-19270.	8.0	147
20	Advanced mechanical properties of graphene paper. Journal of Applied Physics, 2011, 109, .	2.5	146
21	High performance supercapacitor electrode materials based on porous NiCo2O4 hexagonal nanoplates/reduced graphene oxide composites. Chemical Engineering Journal, 2015, 262, 980-988.	12.7	143
22	Hierarchical NiO hollow microspheres assembled from nanosheet-stacked nanoparticles and their application in a gas sensor. RSC Advances, 2012, 2, 4236.	3.6	137
23	Synthesis of reduced graphene oxide/CeO ₂ nanocomposites and their photocatalytic properties. Nanotechnology, 2013, 24, 115603.	2.6	135
24	Ultrathin ZnS Single Crystal Nanowires: Controlled Synthesis and Room-Temperature Ferromagnetism Properties. Journal of the American Chemical Society, 2011, 133, 15605-15612.	13.7	130
25	g-C 3 N 4 /AgBr nanocomposite decorated with carbon dots as a highly efficient visible-light-driven photocatalyst. Journal of Colloid and Interface Science, 2017, 502, 24-32.	9.4	129
26	A novel reduced graphene oxide/Ag/CeO2 ternary nanocomposite: Green synthesis and catalytic properties. Applied Catalysis B: Environmental, 2014, 144, 454-461.	20.2	128
27	Ag nanoparticles decorated MnO2/reduced graphene oxide as advanced electrode materials for supercapacitors. Chemical Engineering Journal, 2014, 252, 95-103.	12.7	127
28	Fabrication of an all solid Z-scheme photocatalyst g-C 3 N 4 /GO/AgBr with enhanced visible light photocatalytic activity. Applied Catalysis A: General, 2017, 539, 104-113.	4.3	124
29	Nickel@Nitrogenâ€Ðoped Carbon@MoS ₂ Nanosheets: An Efficient Electrocatalyst for Hydrogen Evolution Reaction. Small, 2019, 15, e1804545.	10.0	122
30	One-pot solvothermal syntheses and magnetic properties of graphene-based magnetic nanocomposites. Journal of Alloys and Compounds, 2010, 506, 136-140.	5.5	120
31	Reduced graphene oxide supported FePt alloy nanoparticles with high electrocatalytic performance for methanol oxidation. New Journal of Chemistry, 2012, 36, 1774.	2.8	120
32	Concave Co3O4 octahedral mesocrystal: polymer-mediated synthesis and sensing properties. CrystEngComm, 2012, 14, 6264.	2.6	118
33	Preparation and characterization of graphene/CdS nanocomposites. Applied Surface Science, 2010, 257, 747-751.	6.1	113
34	Comparison of Hydrogels Prepared with Ionic-Liquid-Isolated vs Commercial Chitin and Cellulose. ACS Sustainable Chemistry and Engineering, 2016, 4, 471-480.	6.7	100
35	Synthesis of ternary Ag/ZnO/ZnFe2O4 porous and hollow nanostructures with enhanced photocatalytic activity. Applied Catalysis B: Environmental, 2016, 184, 328-336.	20.2	99
36	Advanced Glycation End Product (AGE)-Receptor for AGE (RAGE) Signaling and Up-regulation of Egr-1 in Hypoxic Macrophages. Journal of Biological Chemistry, 2010, 285, 23233-23240.	3.4	95

#	Article	IF	CITATIONS
37	Co3O4/ZnO nanocomposites for gas-sensing applications. Applied Surface Science, 2013, 265, 379-384.	6.1	95
38	The influence of wrinkling in reduced graphene oxide on their adsorption and catalytic properties. Carbon, 2013, 60, 157-168.	10.3	90
39	Facile synthesis of WO3 nanorods/g-C3N4 composites with enhanced photocatalytic activity. Ceramics International, 2015, 41, 5600-5606.	4.8	87
40	Small sized Fe–Co sulfide nanoclusters anchored on carbon for oxygen evolution. Journal of Materials Chemistry A, 2019, 7, 15851-15861.	10.3	87
41	Photochemical deposition of Ag nanocrystals on hierarchical ZnO microspheres and their enhanced gas-sensing properties. CrystEngComm, 2012, 14, 719-725.	2.6	83
42	Metal-organic framework derived Fe/Fe3C@N-doped-carbon porous hierarchical polyhedrons as bifunctional electrocatalysts for hydrogen evolution and oxygen-reduction reactions. Journal of Colloid and Interface Science, 2018, 524, 93-101.	9.4	83
43	Activation of the ROCK1 Branch of the Transforming Growth Factor-Î ² Pathway Contributes to RAGE-Dependent Acceleration of Atherosclerosis in Diabetic ApoE-Null Mice. Circulation Research, 2010, 106, 1040-1051.	4.5	81
44	In situ synthesis of graphene/cobalt nanocomposites and their magnetic properties. Materials Science and Engineering B: Solid-State Materials for Advanced Technology, 2011, 176, 711-715.	3.5	81
45	Cyanide-metal framework derived CoMoO ₄ /Co ₃ O ₄ hollow porous octahedrons as advanced anodes for high performance lithium ion batteries. Journal of Materials Chemistry A, 2018, 6, 1048-1056.	10.3	81
46	Stable aqueous dispersions of graphene prepared with hexamethylenetetramine as a reductant. Journal of Colloid and Interface Science, 2011, 354, 493-497.	9.4	79
47	Morphology syntheses and properties of well-defined Prussian Blue nanocrystals by a facile solution approach. Journal of Colloid and Interface Science, 2009, 329, 188-195.	9.4	78
48	Metal organic framework derived NiFe@N-doped graphene microtube composites for hydrogen evolution catalyst. Carbon, 2017, 116, 68-76.	10.3	77
49	Magnetically recoverable Bi2WO6–Fe3O4 composite photocatalysts: Fabrication and photocatalytic activity. Chemical Engineering Journal, 2012, 200-202, 521-531.	12.7	75
50	Nanocomposites of hematite (α-Fe2O3) nanospindles with crumpled reduced graphene oxide nanosheets as high-performance anode material for lithium-ion batteries. RSC Advances, 2012, 2, 10977.	3.6	75
51	Facile synthesis of nickel–cobalt sulfide/reduced graphene oxide hybrid with enhanced capacitive performance. RSC Advances, 2015, 5, 58777-58783.	3.6	75
52	High-capacity room-temperature hydrogen storage of zeolitic imidazolate framework/graphene oxide promoted by platinum metal catalyst. International Journal of Hydrogen Energy, 2015, 40, 12275-12285.	7.1	69
53	Facile synthesis of Co ₃ O ₄ porous nanosheets/reduced graphene oxide composites and their excellent supercapacitor performance. RSC Advances, 2014, 4, 53180-53187.	3.6	68
54	Porous NiCo2O4 nanosheets/reduced graphene oxide composite: Facile synthesis and excellent capacitive performance for supercapacitors. Journal of Colloid and Interface Science, 2015, 440, 211-218.	9.4	68

#	Article	IF	CITATIONS
55	CN foam loaded with few-layer graphene nanosheets for high-performance supercapacitor electrodes. Journal of Materials Chemistry A, 2015, 3, 7591-7599.	10.3	67
56	Porous CuO superstructure: Precursor-mediated fabrication, gas sensing and photocatalytic properties. Journal of Colloid and Interface Science, 2012, 383, 75-81.	9.4	64
57	Nitrogen-doped carbon dots decorated ultrathin nickel hydroxide nanosheets for high-performance hybrid supercapacitor. Journal of Colloid and Interface Science, 2019, 542, 392-399.	9.4	64
58	Facile synthesis of reduced graphene oxide/CeO2 nanocomposites and their application in supercapacitors. Ceramics International, 2015, 41, 8710-8716.	4.8	63
59	MOF derived nitrogen-doped carbon polyhedrons decorated on graphitic carbon nitride sheets with enhanced electrochemical capacitive energy storage performance. Electrochimica Acta, 2018, 265, 651-661.	5.2	63
60	Preparation and gas-sensing performance of In2O3 porous nanoplatelets. Sensors and Actuators B: Chemical, 2011, 155, 752-758.	7.8	61
61	In situ growth of hollow CuNi alloy nanoparticles on reduced graphene oxide nanosheets and their magnetic and catalytic properties. Applied Surface Science, 2014, 316, 575-581.	6.1	61
62	Assembly of Ag3PO4 nanocrystals on graphene-based nanosheets with enhanced photocatalytic performance. Journal of Colloid and Interface Science, 2013, 405, 1-9.	9.4	59
63	High-performance hybrid supercapacitor realized by nitrogen-doped carbon dots modified cobalt sulfide and reduced graphene oxide. Electrochimica Acta, 2020, 334, 135632.	5.2	59
64	Graphene Oxide Modified Ag ₂ O Nanocomposites with Enhanced Photocatalytic Activity under Visibleâ€Light Irradiation. European Journal of Inorganic Chemistry, 2013, 2013, 6119-6125.	2.0	58
65	Preparation and comparison of bulk and membrane hydrogels based on Kraft- and ionic-liquid-isolated lignins. Green Chemistry, 2016, 18, 5607-5620.	9.0	56
66	An Allâ€Solidâ€State Zâ€Scheme gâ€C ₃ N ₄ /Ag/Ag ₃ VO ₄ Photocatalyst with Enhanced Visibleâ€Light Photocatalytic Performance. European Journal of Inorganic Chemistry, 2017, 2017, 2845-2853.	2.0	56
67	MOF derived CoP-decorated nitrogen-doped carbon polyhedrons/reduced graphene oxide composites for high performance supercapacitors. Dalton Transactions, 2019, 48, 10661-10668.	3.3	55
68	Human Aldose Reductase Expression Accelerates Atherosclerosis in Diabetic Apolipoprotein Eâ^'/â^' Mice. Arteriosclerosis, Thrombosis, and Vascular Biology, 2011, 31, 1805-1813.	2.4	54
69	FeCo nanocrystals encapsulated in N-doped carbon nanospheres/thermal reduced graphene oxide hybrids: Facile synthesis, magnetic and catalytic properties. Carbon, 2014, 77, 255-265.	10.3	54
70	Monodispersed In2O3 mesoporous nanospheres: One-step facile synthesis and the improved gas-sensing performance. Sensors and Actuators B: Chemical, 2015, 220, 977-985.	7.8	54
71	RAGE Suppresses ABCG1-Mediated Macrophage Cholesterol Efflux in Diabetes. Diabetes, 2015, 64, 4046-4060.	0.6	54
72	Synthesis and remarkable capacitive performance of reduced graphene oxide/silver/nickel-cobalt sulfide ternary nanocomposites. Chemical Engineering Journal, 2017, 308, 184-192.	12.7	54

#	Article	IF	CITATIONS
73	Title is missing!. Transition Metal Chemistry, 2002, 27, 372-376.	1.4	53
74	Preparation and characterization of graphene/NiO nanocomposites. Journal of Materials Science, 2011, 46, 1190-1195.	3.7	53
75	Enhanced gas sensing performance of Co-doped ZnO hierarchical microspheres to 1,2-dichloroethane. Sensors and Actuators B: Chemical, 2012, 166-167, 36-43.	7.8	53
76	PKCβ Promotes Vascular Inflammation and Acceleration of Atherosclerosis in Diabetic ApoE Null Mice. Arteriosclerosis, Thrombosis, and Vascular Biology, 2013, 33, 1779-1787.	2.4	53
77	Fe3O4@NiSx/rGO composites with amounts of heterointerfaces and enhanced electrocatalytic properties for oxygen evolution. Applied Surface Science, 2018, 442, 256-263.	6.1	51
78	Hydrothermal synthesis of MnCO3 nanorods and their thermal transformation into Mn2O3 and Mn3O4 nanorods with single crystalline structure. Journal of Alloys and Compounds, 2011, 509, 5672-5676.	5.5	50
79	Carbon coated nickel sulfide/reduced graphene oxide nanocomposites: facile synthesis and excellent supercapacitor performance. Electrochimica Acta, 2014, 146, 525-532.	5.2	50
80	Large-scale facile synthesis of Fe-doped SnO ₂ porous hierarchical nanostructures and their enhanced lithium storage properties. Journal of Materials Chemistry A, 2014, 2, 15875-15882.	10.3	49
81	Synthesis of Cu ₃ P nanocubes and their excellent electrocatalytic efficiency for the hydrogen evolution reaction in acidic solution. RSC Advances, 2016, 6, 9672-9677.	3.6	49
82	Growth of MoS2 nanosheets on M@N-doped carbon particles (MÂ=ÂCo, Fe or CoFe Alloy) as an efficient electrocatalyst toward hydrogen evolution reaction. Chemical Engineering Journal, 2022, 428, 132126.	12.7	49
83	Yolk-shelled ZnO NiO microspheres derived from tetracyanide-metallic-frameworks as bifunctional electrodes for high-performance lithium-ion batteries and supercapacitors. Journal of Power Sources, 2019, 421, 41-49.	7.8	48
84	Double-Network Hierarchical-Porous Piezoresistive Nanocomposite Hydrogel Sensors Based on Compressive Cellulosic Hydrogels Deposited with Silver Nanoparticles. ACS Sustainable Chemistry and Engineering, 2020, 8, 7480-7488.	6.7	48
85	Effect of catalyst loading on hydrogen storage capacity of ZIF-8/graphene oxide doped with Pt or Pd via spillover. Microporous and Mesoporous Materials, 2016, 229, 68-75.	4.4	47
86	Metal-organic framework-derived Co3O4 covered by MoS2 nanosheets for high-performance lithium-ion batteries. Journal of Alloys and Compounds, 2018, 744, 220-227.	5.5	46
87	Controllable Sandwiching of Reduced Graphene Oxide in Hierarchical Defectâ€Rich MoS ₂ Ultrathin Nanosheets with Expanded Interlayer Spacing for Electrocatalytic Hydrogen Evolution Reaction. Advanced Materials Interfaces, 2018, 5, 1801093.	3.7	45
88	Silk-inspired stretchable fiber-shaped supercapacitors with ultrahigh volumetric capacitance and energy density for wearable electronics. Chemical Engineering Journal, 2020, 386, 124024.	12.7	45
89	Loading of Ag on Fe-Co-S/N-doped carbon nanocomposite to achieve improved electrocatalytic activity for oxygen evolution reaction. Journal of Alloys and Compounds, 2019, 773, 40-49.	5.5	44
90	Amorphous CoFe(OH) _x hollow hierarchical structure: an efficient and durable electrocatalyst for oxygen evolution reaction. Catalysis Science and Technology, 2020, 10, 215-221.	4.1	44

#	Article	IF	CITATIONS
91	High energy density hybrid supercapacitor based on cobalt-doped nickel sulfide flower-like hierarchitectures deposited with nitrogen-doped carbon dots. Nanoscale, 2021, 13, 1689-1695.	5.6	44
92	Nitrogen-doped carbon dots modified dibismuth tetraoxide microrods: A direct Z-scheme photocatalyst with excellent visible-light photocatalytic performance. Journal of Colloid and Interface Science, 2018, 531, 473-482.	9.4	43
93	The first cyano-bridged heptanuclear Mn(III)6Fe(III) cluster: crystal structure and magnetic properties of [{Mn(salen)·H2O}6Fe(CN)6][Fe(CN)6]·6H2O. Journal of Molecular Structure, 2003, 657, 325-331.	3.6	42
94	Reversible phase transfer of graphene oxide and its use in the synthesis of graphene-based hybrid materials. Carbon, 2011, 49, 4563-4570.	10.3	42
95	Ionic Liquid Templated Porous Boron-Doped Graphitic Carbon Nitride Nanosheet Electrode for High-Performance Supercapacitor. Electrochimica Acta, 2017, 245, 249-258.	5.2	42
96	Facile microwave-assisted synthesis of monodispersed ball-like Ag@AgBr photocatalyst with high activity and durability. Applied Catalysis A: General, 2013, 455, 183-192.	4.3	41
97	Facile synthesis of magnetically separable reduced graphene oxide/magnetite/silver nanocomposites with enhanced catalytic activity. Journal of Colloid and Interface Science, 2015, 459, 79-85.	9.4	41
98	Nitrogen-doped carbon dot-modified Ag ₃ PO ₄ /GO photocatalyst with excellent visible-light-driven photocatalytic performance and mechanism insight. Catalysis Science and Technology, 2018, 8, 632-641.	4.1	41
99	Polyaniline wrapped graphene functionalized textile with ultrahigh areal capacitance and energy density for high-performance all-solid-state supercapacitors for wearable electronics. Composites Science and Technology, 2020, 198, 108305.	7.8	41
100	Nitrogen-doped carbon dots anchored NiO/Co3O4 ultrathin nanosheets as advanced cathodes for hybrid supercapacitors. Journal of Colloid and Interface Science, 2020, 579, 282-289.	9.4	41
101	Enhanced electrocatalytic performance of Pt-based nanoparticles on reduced graphene oxide for methanol oxidation. Journal of Electroanalytical Chemistry, 2012, 682, 95-100.	3.8	40
102	Porous SnO ₂ –Fe ₂ O ₃ nanocubes with improved electrochemical performance for lithium ion batteries. Dalton Transactions, 2014, 43, 17544-17550.	3.3	40
103	Facile growth of Cu ₂ O hollow cubes on reduced graphene oxide with remarkable electrocatalytic performance for non-enzymatic glucose detection. New Journal of Chemistry, 2017, 41, 9223-9229.	2.8	40
104	Cellulose-derived nitrogen-doped hierarchically porous carbon for high-performance supercapacitors. Cellulose, 2019, 26, 1195-1208.	4.9	40
105	Three-dimensional N-doped graphene/polyaniline composite foam for high performance supercapacitors. Applied Surface Science, 2018, 428, 348-355.	6.1	39
106	Synthesis of graphene oxide-BiPO4 composites with enhanced photocatalytic properties. Applied Surface Science, 2013, 284, 308-314.	6.1	38
107	Anchoring noble metal nanoparticles on CeO2 modified reduced graphene oxide nanosheets and their enhanced catalytic properties. Journal of Colloid and Interface Science, 2014, 432, 57-64.	9.4	38
108	Activating CoFe2O4 electrocatalysts by trace Au for enhanced oxygen evolution activity. Applied Surface Science, 2019, 478, 206-212.	6.1	36

#	Article	IF	CITATIONS
109	Construction of rGOâ€Encapsulated Co ₃ O ₄ â€CoFe ₂ O ₄ Composites with a Doubleâ€Buffer Structure for Highâ€Performance Lithium Storage. Small, 2021, 17, e2101080.	10.0	36
110	Intrinsic Peroxidaseâ€like Activity of Porous CuO Microâ€Inanostructures with Clean Surface. Chinese Journal of Chemistry, 2014, 32, 151-156.	4.9	35
111	In situgrowth of FeNi alloy nanoflowers on reduced graphene oxide nanosheets and their magnetic properties. CrystEngComm, 2012, 14, 1432-1438.	2.6	34
112	Facile synthesis of Mn3O4/reduced graphene oxide nanocomposites with enhanced capacitive performance. Journal of Alloys and Compounds, 2016, 684, 366-371.	5.5	34
113	Protein-derived nitrogen-doped hierarchically porous carbon as electrode material for supercapacitors. Journal of Materials Science: Materials in Electronics, 2018, 29, 12206-12215.	2.2	34
114	Thermal Synthesis of FeNi@Nitrogen-Doped Graphene Dispersed on Nitrogen-Doped Carbon Matrix as an Excellent Electrocatalyst for Oxygen Evolution Reaction. ACS Applied Energy Materials, 2019, 2, 4075-4083.	5.1	34
115	Peroxidase-Like Catalytic Activity of Ag3PO4 Nanocrystals Prepared by a Colloidal Route. PLoS ONE, 2014, 9, e109158.	2.5	32
116	Reduced graphene oxide supported nitrogen-doped porous carbon-coated NiFe alloy composite with excellent electrocatalytic activity for oxygen evolution reaction. Applied Surface Science, 2019, 493, 963-974.	6.1	32
117	Co ₃ ZnC core–shell nanoparticle assembled microspheres/reduced graphene oxide as an advanced electrocatalyst for hydrogen evolution reaction in an acidic solution. Journal of Materials Chemistry A, 2015, 3, 11066-11073.	10.3	31
118	<i>Ager</i> Deletion Enhances Ischemic Muscle Inflammation, Angiogenesis, and Blood Flow Recovery in Diabetic Mice. Arteriosclerosis, Thrombosis, and Vascular Biology, 2017, 37, 1536-1547.	2.4	31
119	Chitosan-assisted synthesis of wearable textile electrodes for high-performance electrochemical energy storage. Cellulose, 2019, 26, 9349-9359.	4.9	31
120	Cuprous sulfide derived CuO nanowires as effective electrocatalyst for oxygen evolution. Applied Surface Science, 2021, 547, 149235.	6.1	31
121	A surface configuration strategy to hierarchical Fe-Co-S/Cu2O/Cu electrodes for oxygen evolution in water/seawater splitting. Applied Surface Science, 2021, 567, 150757.	6.1	31
122	Dissolution-assistant all-in-one synthesis of N and S dual-doped porous carbon for high-performance supercapacitors. Advanced Powder Technology, 2019, 30, 2211-2217.	4.1	30
123	Anchoring nitrogen-doped carbon quantum dots on nickel carbonate hydroxide nanosheets for hybrid supercapacitor applications. Journal of Colloid and Interface Science, 2021, 590, 614-621.	9.4	30
124	Decoration of nickel hexacyanoferrate nanocubes onto reduced graphene oxide sheets as high-performance cathode material for rechargeable aqueous zinc-ion batteries. Journal of Colloid and Interface Science, 2022, 609, 297-306.	9.4	30
125	Sword/scabbard-shaped asymmetric all-solid-state supercapacitors based on PPy-MWCNTs-silk and hollow graphene tube for wearable applications. Chemical Engineering Journal, 2021, 411, 128522.	12.7	29
126	Ge nanoparticles uniformly immobilized on 3D interconnected porous graphene frameworks as anodes for high-performance lithium-ion batteries. Journal of Energy Chemistry, 2022, 69, 161-173.	12.9	29

#	Article	IF	CITATIONS
127	In-situ synthesis of NiS2 nanoparticles/MoS2 nanosheets hierarchical sphere anchored on reduced graphene oxide for enhanced electrocatalytic hydrogen evolution reaction. Journal of Colloid and Interface Science, 2022, 624, 150-159.	9.4	29
128	Facile electrochemical synthesis of CeO2@Ag@CdS nanotube arrays with enhanced photoelectrochemical water splitting performance. Dalton Transactions, 2015, 44, 19935-19941.	3.3	27
129	Belt-like nickel hydroxide carbonate/reduced graphene oxide hybrids: Synthesis and performance as supercapacitor electrodes. Colloids and Surfaces A: Physicochemical and Engineering Aspects, 2018, 538, 748-756.	4.7	27
130	An Electrocatalyst for a Hydrogen Evolution Reaction in an Alkaline Medium: Threeâ€Dimensional Graphene Supported CeO ₂ Hollow Microspheres. European Journal of Inorganic Chemistry, 2018, 2018, 3952-3959.	2.0	27
131	In-situ synthesis of Ge/reduced graphene oxide composites as ultrahigh rate anode for lithium-ion battery. Journal of Alloys and Compounds, 2019, 801, 90-98.	5.5	27
132	Enhanced heavy metal adsorption ability of lignocellulosic hydrogel adsorbents by the structural support effect of lignin. Cellulose, 2019, 26, 4005-4019.	4.9	27
133	Cyanometallic frameworks derived hierarchical porous Fe 2 O 3 /NiO microflowers with excellent lithium-storage property. Journal of Alloys and Compounds, 2017, 698, 469-475.	5.5	26
134	Ionic liquid directed construction of foam-like mesoporous boron-doped graphitic carbon nitride electrode for high-performance supercapacitor. Journal of Colloid and Interface Science, 2018, 532, 261-271.	9.4	26
135	Facile synthesis and gas-sensing performance of Sr- or Fe-doped In ₂ O ₃ hollow sub-microspheres. RSC Advances, 2015, 5, 64228-64234.	3.6	25
136	Construction of magnetically separable Ag3PO4/Fe3O4/GO composites as recyclable photocatalysts. Ceramics International, 2015, 41, 13509-13515.	4.8	25
137	Spatial Analysis of Regional Factors and Lung Cancer Mortality in China, 1973–2013. Cancer Epidemiology Biomarkers and Prevention, 2017, 26, 569-577.	2.5	25
138	Bimetallic metal-organic framework derived Sn-based nanocomposites for high-performance lithium storage. Electrochimica Acta, 2019, 323, 134855.	5.2	25
139	Ni3S2 nanostrips@FeNi-NiFe2O4 nanoparticles embedded in N-doped carbon microsphere: An improved electrocatalyst for oxygen evolution reaction. Journal of Colloid and Interface Science, 2022, 617, 1-10.	9.4	25
140	ZnNi alloy nanoparticles grown on reduced graphene oxide nanosheets and their magnetic and catalytic properties. RSC Advances, 2014, 4, 386-394.	3.6	24
141	Flower-like silver bismuthate supported on nitrogen-doped carbon dots modified graphene oxide sheets with excellent degradation activity for organic pollutants. Journal of Colloid and Interface Science, 2019, 540, 167-176.	9.4	24
142	One step in-situ synthesis of Ni3S2/Fe2O3/N-doped carbon composites on Ni foam as an efficient electrocatalyst for overall water splitting. Applied Surface Science, 2020, 527, 146918.	6.1	24
143	Cyanide-metal framework derived porous MoO3-Fe2O3 hybrid micro- octahedrons as superior anode for lithium-ion batteries. Chemical Engineering Journal, 2021, 426, 130347.	12.7	24
144	Self-templated formation of hierarchically yolk–shell-structured ZnS/NC dodecahedra with superior lithium storage properties. Nanoscale, 2021, 13, 1988-1996.	5.6	24

#	Article	IF	CITATIONS
145	Dual functionalized Fe2O3 nanosheets and Co9S8 nanoflowers with phosphate and nitrogen-doped carbon dots for advanced hybrid supercapacitors. Chemical Engineering Journal, 2022, 450, 137942.	12.7	24
146	One-step construction of ZnS/C and CdS/C one-dimensional core–shell nanostructures. Journal of Materials Chemistry, 2007, 17, 1326-1330.	6.7	23
147	Nitrogen-doped carbon composites derived from 7,7,8,8-tetracyanoquinodimethane-based metal–organic frameworks for supercapacitors and lithium-ion batteries. RSC Advances, 2017, 7, 25182-25190.	3.6	23
148	One-step thermal synthesis of nickel nanoparticles modified graphene sheets for enzymeless glucose detection. Journal of Colloid and Interface Science, 2017, 506, 678-684.	9.4	23
149	Graphene oxide-FePO4 nanocomposite: Synthesis, characterization and photocatalytic properties as a Fenton-like catalyst. Ceramics International, 2018, 44, 7240-7244.	4.8	23
150	Bismuth oxide/nitrogen-doped carbon dots hollow and porous hierarchitectures for high-performance asymmetric supercapacitors. Advanced Powder Technology, 2020, 31, 632-638.	4.1	23
151	Scalable surface engineering of commercial metal foams for defect-rich hydroxides towards improved oxygen evolution. Journal of Materials Chemistry A, 2020, 8, 12603-12612.	10.3	23
152	Muscle-inspired capacitive tactile sensors with superior sensitivity in an ultra-wide stress range. Journal of Materials Chemistry C, 2020, 8, 5913-5922.	5.5	23
153	Metal-organic frameworks-derived carbon modified wood carbon monoliths as three-dimensional self-supported electrodes with boosted electrochemical energy storage performance. Journal of Colloid and Interface Science, 2022, 620, 376-387.	9.4	23
154	Controlled synthesis and gas sensing properties of porous Fe ₂ O ₃ /NiO hierarchical nanostructures. CrystEngComm, 2015, 17, 5522-5529.	2.6	22
155	Morphological synthesis of Prussian blue analogue Zn 3 [Fe(CN) 6] 2 â‹ x H 2 O micro-/nanocrystals and their excellent adsorption performance toward methylene blue. Journal of Colloid and Interface Science, 2016, 464, 191-197.	9.4	22
156	Optical Properties and a Simple and General Route for the Rapid Syntheses of Reduced Graphene Oxide–Metal Sulfide Nanocomposites. European Journal of Inorganic Chemistry, 2013, 2013, 256-262.	2.0	21
157	Facile synthesis and enhanced catalytic performance of reduced graphene oxide decorated with hexagonal structure Ni nanoparticles. Journal of Colloid and Interface Science, 2017, 487, 223-230.	9.4	21
158	<i>110th Anniversary:</i> High-Molecular-Weight Chitin and Cellulose Hydrogels from Biomass in Ionic Liquids without Chemical Crosslinking. Industrial & Engineering Chemistry Research, 2019, 58, 19862-19876.	3.7	21
159	Carbon cloth supported graphitic carbon nitride nanosheets as advanced binder-free electrodes for supercapacitors. Journal of Electroanalytical Chemistry, 2020, 873, 114390.	3.8	21
160	H2SO4-assisted tandem carbonization synthesis of PANI@carbon@textile flexible electrode for high-performance wearable energy storage. Applied Surface Science, 2021, 535, 147755.	6.1	21
161	Reduced graphene oxide uniformly decorated with Co nanoparticles: facile synthesis, magnetic and catalytic properties. RSC Advances, 2016, 6, 107709-107716.	3.6	20
162	Small molecular amine mediated synthesis of hydrophilic CdS nanorods and their photoelectrochemical water splitting performance. Dalton Transactions, 2015, 44, 1465-1472.	3.3	19

#	Article	IF	CITATIONS
163	Organic–inorganic hybrid ZnS(butylamine) nanosheets and their transformation to porous ZnS. Journal of Colloid and Interface Science, 2016, 468, 136-144.	9.4	19
164	Nitrogen-enriched carbon spheres coupled with graphitic carbon nitride nanosheets for high performance supercapacitors. Dalton Transactions, 2018, 47, 9724-9732.	3.3	19
165	Type-I superconductivity in <mml:math xmlns:mml="http://www.w3.org/1998/Math/MathML"><mml:mrow><mml:msub><mml:mi>Al</mml:mi><mml:mi Physical Review B, 2019, 99, .</mml:mi </mml:msub></mml:mrow></mml:math 	n>\$62/mm	l:m19>
166	Shape- and size-controlled synthesis of coordination polymer {[Cu(en)2][KFe(CN)6]}n nano/micro-crystals. Journal of Materials Science, 2009, 44, 6447-6450.	3.7	18
167	In-situ growth of Cu nanoparticles on reduced graphene oxide nanosheets and their excellent catalytic performance. Ceramics International, 2015, 41, 4056-4063.	4.8	18
168	Polymer guided synthesis of Ni(OH)2 with hierarchical structure and their application as the precursor for sensing materials. CrystEngComm, 2013, 15, 9189.	2.6	17
169	Syntheses, Crystal Structures, and Magnetic Properties of Four New Cyano-Bridged Bimetallic Complexes Based on the mer-[FeIII(qcq)(CN)3]â^' Building Block. Inorganic Chemistry, 2014, 53, 116-127.	4.0	17
170	Structures for the 3d–5d–4f Heterotrimetallic Complexes: Synthesis, Structures, and Magnetic Properties. European Journal of Inorganic Chemistry, 2017, 2017, 3946-3952.	2.0	17
171	Hierarchical flower-like architecture of nickel phosphide anchored with nitrogen-doped carbon quantum dots and cobalt oxide for advanced hybrid supercapacitors. Journal of Colloid and Interface Science, 2022, 609, 503-512.	9.4	17
172	Hydrothermal syntheses of silver phosphate nanostructures and their photocatalytic performance for organic pollutant degradation. Crystal Research and Technology, 2014, 49, 975-981.	1.3	16
173	Nitrogen and sulfur co-doped carbon sub-micrometer sphere-based electrodes toward high-performance hybrid supercapacitors. Applied Surface Science, 2022, 590, 153121.	6.1	15
174	Low dimensional cyano-bridged heterobimetallic M–FeIII(M = NiII, CuII) complexes constructed from Mer-[FeIII(qcq)(CN)3]â~'building blocks: syntheses, structures and magnetic properties. RSC Advances, 2014, 4, 61-70.	3.6	14
175	Construction of Ni ^{II} Ln ^{III} M ^{III} (Ln = Gd ^{III} ,) Tj ETQq1 1 0.78431 Dalton Transactions, 2015, 44, 20193-20199.	4 rgBT /O 3.3	verlock 10 14
176	Construction of copper(II)–dysprosium(III)–iron(III) trinuclear cluster based on Schiff base ligand: Synthesis, structure and magnetism. Inorganica Chimica Acta, 2015, 437, 188-194.	2.4	14
177	Fast growth of highly ordered porous alumina films based on closed bipolar electrochemistry. Electrochemistry Communications, 2020, 119, 106822.	4.7	14
178	Oneâ€Pot Hydrothermal Synthesis of Ni ₃ S ₂ /MoS ₂ /FeOOH Hierarchical Microspheres on Ni Foam as a Highâ€Efficiency and Durable Dualâ€Function Electrocatalyst for Overall Water Splitting. ChemElectroChem, 2021, 8, 665-674.	3.4	14
179	Nickel sulfide and cobalt sulfide nanoparticles deposited on ultrathin carbon two-dimensional nanosheets for hybrid supercapacitors. Applied Surface Science, 2022, 574, 151727.	6.1	14
180	Syntheses, crystal structures and magnetic properties of two low-dimensional cyano-bridged CrIII–MnII/III assemblies. New Journal of Chemistry, 2012, 36, 1180.	2.8	13

#	Article	IF	CITATIONS
181	Synthesis of AgCl hollow cubes and their application in photocatalytic degradation of organic pollutants. CrystEngComm, 2015, 17, 2517-2522.	2.6	13
182	Anchoring of Ag nanoparticles on Fe3O4 modified polydopamine sub-micrometer spheres with enhanced catalytic activity. Applied Surface Science, 2018, 462, 1-7.	6.1	13
183	The Influence of dâ€f Coupling on Slow Magnetic Relaxation in Ni ^{II} Ln ^{III} M ^{III} (Ln = Gd, Tb, Dy; M = Cr, Fe, Co) Clusters. European Journal of Inorganic Chemistry, 2019, 2019, 2361-2367.	2.0	13
184	Three-dimensional graphene network deposited with mesoporous nitrogen-doped carbon from non-solvent induced phase inversion for high-performance supercapacitors. Journal of Colloid and Interface Science, 2020, 558, 21-31.	9.4	13
185	Highly monodispersed Fe2WO6 micro-octahedrons with hierarchical porous structure and oxygen vacancies for lithium storage. Chemical Engineering Journal, 2021, 413, 127504.	12.7	13
186	<i>In Situ</i> Electrochemical Activation of Fe/Co-Based 8-Hydroxyquinoline Nanostructures on Copper Foam for Oxygen Evolution. ACS Applied Nano Materials, 2021, 4, 9409-9417.	5.0	13
187	FeNi@Nâ€Doped Graphene Core–Shell Nanoparticles on Carbon Matrix Coupled with MoS ₂ Nanosheets as a Competent Electrocatalyst for Efficient Hydrogen Evolution Reaction. Advanced Materials Interfaces, 2022, 9, .	3.7	13
188	Microrods based on nanocubes of Prussian blue. Applied Surface Science, 2009, 255, 9182-9185.	6.1	12
189	Platelet-like nickel hydroxide: Synthesis and the transferring to nickel oxide as a gas sensor. Journal of Colloid and Interface Science, 2013, 412, 100-106.	9.4	12
190	αâ€Fe ₂ O ₃ nanospindles loaded with ZnO nanocrystals: Synthesis and improved gas sensing performance. Crystal Research and Technology, 2014, 49, 452-459.	1.3	12
191	New examples of hetero-tri-metallic complexes Cull-LnIII-MIII (M = Cr, Fe; Ln = Gd, Dy, Er): Synthesis, structures and magnetic properties. Inorganica Chimica Acta, 2016, 453, 482-487.	2.4	12
192	Cyanometallic framework-derived dual-buffer structure of Sn-Co based nanocomposites for high-performance lithium storage. Journal of Alloys and Compounds, 2020, 830, 154680.	5.5	12
193	Hierarchical ZnO microspheres built by sheet-like network: Large-scale synthesis and structurally enhanced catalytic performances. Materials Chemistry and Physics, 2012, 132, 1065-1070.	4.0	11
194	Reduced graphene oxide/CoSe2 nanocomposites: hydrothermal synthesis and their enhanced electrocatalytic activity. Journal of Materials Science, 2013, 48, 7913-7919.	3.7	11
195	Syntheses, crystal structures and magnetic properties of four cyano-bridged bimetallic alternating chain complexes based on [CrIII(salen)(CN)2]â~ and [CrIII(bipy)(CN)4]â~ building blocks. New Journal of Chemistry, 2013, 37, 941.	2.8	11
196	One-pot synthesis of PrPO4 nanorods–reduced graphene oxide composites and their photocatalytic properties. New Journal of Chemistry, 2014, 38, 2305.	2.8	11
197	Synthesis of GO–AglO4 nanocomposites with enhanced photocatalytic efficiency in the degradation of organic pollutants. Journal of Materials Science, 2017, 52, 6100-6110.	3.7	11
198	RAGE Mediates Cholesterol Efflux Impairment in Macrophages Caused by Human Advanced Glycated Albumin. International Journal of Molecular Sciences, 2020, 21, 7265.	4.1	11

#	Article	IF	CITATIONS
199	A flexible hydrogel tactile sensor with low compressive modulus and dynamic piezoresistive response regulated by lignocellulose/graphene aerogels. Journal of Materials Chemistry C, 2021, 9, 12895-12903.	5.5	11
200	Heterotrimetallic Cu ^{II} (L)–Ln ^{III} –M ^{III} (M = Cr, Fe; Ln = Pr, Nd, Sm, Gd) Complexes Ranging from 0D Clusters to 1D Chains and 2D Networks: Syntheses, Structures, and Magnetism. European Journal of Inorganic Chemistry, 2016, 2016, 4921-4927.	2.0	10
201	Loading of individual Se-doped Fe ₂ O ₃ -decorated Ni/NiO particles on carbon cloth: facile synthesis and efficient electrocatalysis for the oxygen evolution reaction. Dalton Transactions, 2020, 49, 15682-15692.	3.3	10
202	Size-controllable synthesis of Zn2GeO4 hollow rods supported on reduced graphene oxide as high-capacity anode for lithium-ion batteries. Journal of Colloid and Interface Science, 2021, 589, 13-24.	9.4	10
203	Morphology-Dependent Electrocatalytic Performance of a Two-Dimensional Nickel–Iron MOF for Oxygen Evolution Reaction. Inorganic Chemistry, 2022, 61, 7095-7102.	4.0	10
204	Syntheses, Crystal Structures, and Magnetic Properties of Two Cyanoâ€Bridged Cr ^{III} M ^{II} (M = Cu, Ni) Bimetallic Assemblies with Macrocyclic Ligands. European Journal of Inorganic Chemistry, 2012, 2012, 5050-5057.	2.0	9
205	The orbital characters of low-energy electronic structure in iron-chalcogenide superconductor K x Fe2â^'y Se2. Science Bulletin, 2012, 57, 3829-3835.	1.7	9
206	Morphological syntheses of ZnO nanostructures under microwave irradiation. Journal of Materials Science, 2013, 48, 2358-2364.	3.7	9
207	Fabrication of highly ordered porous anodic alumina films in 0.75 M oxalic acid solution without using nanoimprinting. Materials Research Bulletin, 2019, 111, 24-33.	5.2	9
208	Carbon Cloth Supported Nitrogen Doped Porous Carbon Wrapped Co Nanoparticles for Effective Overall Water Splitting. ChemCatChem, 2021, 13, 2158-2166.	3.7	9
209	One-pot synthesis of Ni3S2/Co3S4/FeOOH flower-like microspheres on Ni foam: An efficient binder-free bifunctional electrode towards overall water splitting. Colloids and Surfaces A: Physicochemical and Engineering Aspects, 2021, 631, 127689.	4.7	9
210	A facile and general route for the synthesis of semiconductor quantum dots on reduced graphene oxide sheets. RSC Advances, 2014, 4, 13601.	3.6	8
211	Co–Fe Bimetal Phosphate Composite Loaded on Reduced Graphene Oxide for Oxygen Evolution. Nano, 2019, 14, 1950003.	1.0	8
212	Controlled synthesis of [Fe(pyridine)2Ni(CN)4] nanostructures and their shape-dependent spin-crossover properties. Journal of Magnetism and Magnetic Materials, 2020, 496, 165938.	2.3	8
213	Folic acid mediated synthesis of hierarchical ZnO micro-flower with improved gas sensing properties. Advanced Powder Technology, 2020, 31, 2227-2234.	4.1	8
214	Facile synthesis of novel tungsten-based hierarchical core-shell composite for ultrahigh volumetric lithium storage. Journal of Colloid and Interface Science, 2020, 567, 28-36.	9.4	8
215	Synthesis, Structure and Characterization of the Cyano-Bridged Heteropolymer Poly{[Bis(Trimethylenediamine)Copper(II)][Hexacyanocobalt(III)]} Perchlorate Dihydrate with a Two-Dimensional Framework. Journal of Coordination Chemistry, 2002, 55, 1191-1198.	2.2	7
216	Coordination polymer micro/nano-crystals: controlled synthesis and formation mechanism in the case of Mn2Mo(CN)8·xH2O. CrystEngComm, 2013, 15, 2909.	2.6	7

#	Article	IF	CITATIONS
217	One-pot synthesis, formation mechanism and near-infrared fluorescent properties of hollow and porous α-mercury sulfide. CrystEngComm, 2013, 15, 4162.	2.6	7
218	Fabrication of N-doped Reduced Graphene Oxide/Ag ₃ PO ₄ Nanocomposite with Excellent Photocatalytic Activity for the Degradation of Organic Pollutants. Nano, 2017, 12, 1750013.	1.0	7
219	Templated preparation of hierarchically porous nitrogen-doped carbon electrode material via a mild phase inversion route for high-performance supercapacitor. Journal of Energy Storage, 2020, 32, 101854.	8.1	7
220	Template-assisted synthesis of accordion-like CoFe(OH) nanosheet clusters on GO sheets for electrocatalytic water oxidation. Journal of Electroanalytical Chemistry, 2022, 905, 115957.	3.8	7
221	Structures and magnetic studies of two new bimetallic chain complexes constructed by manganese(III)–(Schiff-base) and mer-tricyanidoferrate building block. Inorganica Chimica Acta, 2014, 414, 53-58.	2.4	6
222	Low temperature synthesis of spindleâ€like ZnO nanostructures under microwave irradiation. Crystal Research and Technology, 2013, 48, 1022-1026.	1.3	5
223	Shape and Size Tunable Synthesis of Coordination Polymer Mn ₂ W(CN) ₈ · <i>x</i> H ₂ O Microcrystals through a Simple Solution Chemical Route. European Journal of Inorganic Chemistry, 2013, 2013, 5297-5302.	2.0	5
224	Tuning the structures of manganese(III) (Schiff base) complexes: Syntheses, crystal structures and magnetic properties. Inorganica Chimica Acta, 2014, 423, 115-122.	2.4	5
225	Fabrication of ZIF-8@SF Linear Composite Through Directly Feeding Approach. Journal of Inorganic and Organometallic Polymers and Materials, 2019, 29, 2083-2089.	3.7	5
226	NiFeâ€NiFe 2 O 4 /rGO composites: Controlled preparation and superior lithium storage properties. Journal of the American Ceramic Society, 2021, 104, 6696.	3.8	5
227	An effective Fe/Co tripolyphosphate pre-catalyst for oxygen evolution with alkaline electrolyte. Applied Surface Science, 2022, 575, 151761.	6.1	5
228	Flower-like nickel‑cobalt-layered double hydroxide nanosheets deposited on hierarchically porous graphitic carbon nitride for enhanced electrochemical energy storage. Journal of Energy Storage, 2022, 51, 104541.	8.1	5
229	Syntheses, crystal structures and magnetic properties of three cyano-bridged trinuclear clusters based on modified hexacyanometalates building blocks. Inorganica Chimica Acta, 2013, 402, 97-103.	2.4	4
230	Fe3+–Co2+ species loaded on carbon as an effective pre-catalyst for oxygen evolution. New Journal of Chemistry, 2020, 44, 21326-21331.	2.8	4
231	REGIONAL VARIATIONS AND CHANGES IN INDUSTRIAL PRODUCTIVITY IN CHINA, 1980–1995. Asian Geographer, 2001, 20, 53-78.	1.0	3
232	Incorporation of Fe/Co species on carbon: A facile strategy for boosting oxygen evolution. Inorganic Chemistry Communication, 2020, 111, 107674.	3.9	3
233	Electronic structure and signature of Tomonaga–Luttinger liquid state in epitaxial CoSb1â^'x nanoribbons. Npj Quantum Materials, 2021, 6, .	5.2	3
234	Physical properties of noncentrosymmetric tungsten and molybdenum aluminides. Physical Review Materials, 2018, 2, .	2.4	3

#	Article	IF	CITATIONS
235	Topological surface states in superconducting <mml:math xmlns:mml="http://www.w3.org/1998/Math/MathML"> <mml:msub> <mml:mi> CaBi </mml:mi> <mml:mn> 2 Physical Review B, 2021, 104, .</mml:mn></mml:msub></mml:math 	n a. 2 <td>l:masub></td>	l:masub>
236	Synthesis of CdII–4,4′-bipy coordination polymer nanorods with tunable size and shape. Physica E: Low-Dimensional Systems and Nanostructures, 2008, 41, 101-105.	2.7	2
237	<i>N</i> -(Quinolin-8-yl)quinoline-2-carboxamide. Acta Crystallographica Section E: Structure Reports Online, 2012, 68, o1688-o1688.	0.2	2
238	Superconductivity induced by U doping in the SmFeAsO system. Physical Review B, 2013, 87, .	3.2	2
239	Ag ₂ S – CoS ₂ hetero-nanostructures: One-pot colloidal synthesis and improved magnetic properties. Functional Materials Letters, 2014, 07, 1450024.	1.2	2
240	Crystal structures and magneto-structural correlation analysis for several cyano-bridged bimetallic complexes based on Mn ^{III} –Fe ^{III} systems. New Journal of Chemistry, 2014, 38, 5925-5934.	2.8	2
241	Low dimensional magnetic assemblies based on MnIII(Schiff base) and/or Mer-tricyanidoferrate building blocks: Syntheses, crystal structures and magnetic properties. Polyhedron, 2015, 85, 457-466.	2.2	2
242	Synthesis, structure and magnetic properties of two new 3d-3d′-4f clusters of NillHollIMIII (M = Fe, Co). Inorganica Chimica Acta, 2018, 482, 687-690.	2.4	2
243	Bimetallic and trimetallic chains of Fe-CN-Ln complexes: Synthesis, structural characterization, and magnetic properties. Inorganica Chimica Acta, 2021, 516, 120119.	2.4	2
244	Zn-assisted self-assembly synthesis of graphene/multi-walled carbon nanotubes hybrid films for high-performance wearable supercapacitors. Materials Chemistry and Physics, 2022, 290, 126515.	4.0	2
245	The Influence of Location on Rural Industrial Development in Beijing Suburbs : A GIS Analysis. Annals of GIS, 2000, 6, 81-96.	3.1	1
246	Nodeless superconducting gaps in Ca10(Pt4-δAs8)((Fe1-x Pt x)2As2)5 probed by quasiparticle heat transport. Science China: Physics, Mechanics and Astronomy, 2016, 59, 1.	5.1	1
247	Analysis of Forty Years of Geographic Disparity in Liver Cancer Mortality and the Influence of Risk Factors. Annals of the American Association of Geographers, 0, , 1-18.	2.2	1
248	A Wet Impregnation Strategy for Advanced FeNiâ€Based Electrocatalysts towards Oxygen Evolution. European Journal of Inorganic Chemistry, 2021, 2021, 139-146.	2.0	1
249	catena-Poly[[bis(dicyanamido-κN1)cobalt(II)]bis{μ-1,2-bis[(1,2,4-triazol-1-yl)methyl]benzene-κ2N4:N4′}]. Ac Crystallographica Section E: Structure Reports Online, 2014, 70, m244-m244.	^{:a} 0.2	0
	\mathbf{D} : $\hat{1}$ / $\hat{\mathbf{n}}$ and $\hat{\mathbf{n}}$	انسم ۲ میں	

250 Di-Î¹/4-cyanido-tetracyanido(5,5,7,12,12,14-hexamethyl-1,4,8,11-tetraazacyclotetradecane)[N-(quinolin-8-yl)quinoline-2-carboxamidato] 2.07-hydrate. Acta Crystallographica Section E: Structure Reports Online, 2013, 69, m271-m272.